Europium doped nanophosphors and applications in *in vitro* optical bioimaging

Anuradha and Indrajit Roy[*]

Department of Chemistry, University of Delhi, Delhi-110007, India.

ABSTRACT

We report the synthesis of 'rare-earth' doped calcium phosphate-based 'nanophosphors' in a methanolic medium, with surface modified with trisilanol. In order to enhance the luminescence intensity of these nanophosphors, 1, 10-phenanthroline was used as a co-dopant. The synthesized nanoparticles were characterized for various physical properties. In vitro analyses showed that the particles were taken up by cells, without any sign of cytotoxicity. Using fluorescence microscopy and cell uptake studies, we have demonstrated the enhanced luminescence intensity of nanophosphors when 1, 10- phenanthroline was used. These results highlight the potential for nanophosphors to be used in safe and efficient optical bioimaging.

Keywords: Nanophosphors, 1, 10-phenanthroline, co-dopant, emission, optical bioimaging

INTRODUCTION

Nanophosphors, classically solid inorganic nanosized materials doped with rare-earth ions, have received extensive consideration during the past few years due to their unique optical properties, different from those observed in bulk phosphors. Non-radiative relaxation process and spatial confinement in nanophosphors are responsible for their unique optical nature.[1] Typically, nanosize phosphor particles with size close to or below 100 nm, having a spherical shape, are strongly desired for their applications in high resolution display devices.[2] Significant differences are expected from the confinement effects on nanophosphor, which affect their luminescence efficiency and photodynamics.[3] The luminescence efficiency of phosphors used for optical applications mainly depends on the physical characteristics of the prepared phosphors, such as their particle size,[4] surface morphology,[5] concentration quenching,[6] and crystallinity.[7]

When the external photon sources are used for excitation of the phosphor, a phosphorescence process (light absorption, excitation, relaxation, and emission) takes places in the material. The photon energy is absorbed by either the host material or is directly absorbed on impurity atom; the absorbed energy on host atom is transferred to the impurity atom (so-called activators). As a result of that, the activators emit visible light by relaxation of photoexcited electron to lower energy state. In most cases, the emission of photon from phosphors is generated from impurities.

In the light emission (phosphorescence) process of the rare-earth doped phosphor materials, the color of the emitting light from phosphor materials depends on the type of doping impurities in the host. In order to get high photoluminescence in nanophosphor particles, large amount of exciting energy should be absorbed by the activator and concurrently the excitations return to the ground state by the radiative process. The 4f electronic states originated from rare-earth ions contained in the nanophosphor particles is highly localized and is not altered by reduced size of phosphors.

Because of the small forced dipole strength of f-f transition, direct excitation to the 4f excited state of lanthanide complexes is not efficient. An alternative is to employ an organic chromophore as a good light absorber to sensitize lanthanide ions (Ln^{3+}) by energy transfer, usually from the triplet state, by the antenna effect.[8-11] The ligand 1, 10-phenanthroline (PA) is an excellent antenna with singlet and triplet states at 29200 and 22100 cm^{-1}, respectively, and has been employed to sensitize various Ln^{3+} species in crystals and hybrid materials.[12-14] These unique properties can widen nanophosphors use to many potential applications such as optical, electrical, medical and biological technologies.

In this work, doped calcium phosphate-based nanophosphors were synthesized in a methanolic medium, with surface modified using trisilanol. 1, 10- phenanthroline

Dr.Indrajit Roy
Department of Chemistry, University of Delhi, Delhi-110007, India.
Tel: +11-9560721851 Email: indrajitroy11@gmail.com

----

http://pubs.iscience.in/jist

Journal of Integrated Science and Technology

J. Integr. Sci. Technol., 2016, 4(2), 46-50   1

was used as a co-dopant in order to enhance the luminescence intensity of these nanophosphors. After synthesis in methanol, the resulting nanophosphors were characterized for their size, functionality and crystallinity. Following physical and optical characterization of these nanophosphors, we have investigated their interaction with cultured cancer cells in vitro, beginning with visualization their cellular uptake and intra cellular localization using fluorescence microscopy. We have demonstrated the enhanced intensity of nanophosphors when 1, 10-phenanthroline was used as a co-dopant, which is successfully shown by fluorescence microscopy and cell uptake studies.

MATERIALS

Calcium chloride, disodium hydrogen phosphate, sodium hydroxide, methanol, Europium (III) nitrate hexahydrate, 1, 10-phenanthroline and tetrahydrofuran (THF) were purchased from SRL (India). Tris-HCl buffer and Triton X-100 were purchased from Sigma-Aldrich (USA). Cell culture media (DMEM), fetal bovine serum (FBS), antibiotics (penicillin and streptomycin), amphotericin B, and MTT Reagent [3-(4, 5-dimethylthiazol-2-yl)-2, 5-diphenyltetrazolium bromide] were obtained from Genetix (India). Human lung cancer A-549 cells were purchased from ATCC (USA). All chemicals were used without any further purification. Unless otherwise mentioned, the experiments were carried out at ambient temperature and pressure. The water used for reactions is doubly distilled.

METHODS

Synthesis of doped calcium phosphate nanophosphors

Trisilanol [(c-C_5H_9)$_7$Si$_7$O$_9$ (OH)$_3$] was prepared according to previously reported method 15. Sodium hydroxide was added to 45 ml of a methanolic solution of the prepared trisilanol (feed molar ratio of sodium hydroxide to trisilanol was 3:1). After that, to the resulting solution of sodium trisilanolate in methanol, 1.5 ml of each aqueous reactant solutions (0.05 M CaCl$_2$ and 0.0175 M Na$_2$HPO$_4$), and 20% (Eu^{2+}:Ca^{2+}) were added via syringe at 30°C under N$_2$ atmosphere. For synthesis of nanophosphors with enhanced intensity, 1, 10-phenanthroline (PA) was added as a co-dopant in the solution. Appearance of translucency in the solution indicated the formation of nanoparticles. This solution was kept at 30°C under N$_2$ atmosphere for 24 hours with gentle stirring for the completion of the reaction. The resulting, doped calcium phosphate nanophosphors were separated by centrifugation (10,000 rpm, 5 min), and washed three times with pure methanol. Finally, the precipitate was dried in a vacuum oven at 50°C for one day. The nanoparticles were further purified by suspending the precipitate in THF by vigorous stirring, followed by separation by centrifugation (10,000 rpm, 5 min). Finally, dried nanoparticles were dispersed in water for further studies.

CHARACTERIZATION

The The size of the doped calcium phosphate nanoparticles was determined using Transmission electron microscopy (TEM). Aqueous dispersion of nanoparticles were sonicated, drop-coated and dried onto formvar coated 200 mesh copper grids (Ted Pella, USA), followed by imaging using a TECNAI G2-30 U TWIN TEM instrument (FEI, Eindhoven, The Netherlands), with an acceleration voltage of 300 kV. High resolution powder X-ray diffraction (HXRD) was used to analyze the phase composition of the nanoparticles, using a Brukar D8 Discover X-ray spectrometer, over the 2θ range from 20–600, with a step size of 0.020, scan rate of 1.5 second/step, 40 milliamp current and 40KV voltage, using Cu-Kα radiation (λ= 1.54060 A˚). The Fourier transform infrared spectroscopy (FTIR) spectra for the prepared nanoparticles were recorded on Perkin Elmer RX1 Instrument. The optical properties (excitation and photoluminescence emission spectra) of the nanoparticles were recorded using a Cary Eclipse fluorescence spectrometer (Varian, Palo Alto, CA).

IN VITRO STUDIES:

The The human lung cancer cells A-549 were grown in DMEM media, supplemented with 10% fetal bovine serum (FBS), 1% antibiotic penicillin/streptomycin, and 1% antifungal Amphotericin B. The cells were maintained at 37 °C and 5% CO$_2$ in a humidified incubator, using standard cell culture procedures and manufacturer's instructions. For analyzing cell viability upon treatment with nanophosphors (CP-EU, CP-EU-PA), one day prior to treatment, and these cells were trypsinized and resuspended in fresh media. 75,000 cells/ ml fresh media were added to each well of a sterilized 24-well plate, and transferred back to the incubator for attachment and overnight growth. Next day, to the cells at a confluency of about 50%, aqueous dispersions of the nanoparticles were added, mixed by swirling, and transferred back to the incubator.

After two days of incubation, the plate was taken out, and the cells in each well were washed three times with sterile PBS, and treated with 100 µl of MTT reagent [3-(4,5-dimethylthiazol-2-yl)-2,5-diphenyltetrazolium bromide, (5 mg/ml in PBS)] for 2 hours [16]. The resulting blue-coloured formazan crystals were dissolved in DMSO, and the optical density of this solution was recorded at 570 nm using UV–visible spectrophotometry. The optical density of each solution reflected the viability of the cells in each well. The percentage viability of the treated cells were calculated after comparing their optical density with that of non-treated cells (positive control), the later being arbitrarily assigned 100 % viability. The experiment was carried out in triplicates.

Fluorescence microscopy of cells and fluorescence estimation from cell lysates were used to monitor the uptake of the nanophosphors (CP-EU, CP-EU-PA) in cells. One day prior to treatment, the cells were seeded in sterilized 6-well plates (2, 00,000 cells/2 ml fresh media in each well) and returned to the incubator. Next day, to the cells at a confluency of about 70%, aqueous dispersion of nanophosphors (CP-EU, CP-EU-PA) were added (nanophosphor concentration 100 µg/ml), mixed by swirling, and returned to the incubator. After two hours of incubation, the plate was taken out; the treatment-media aspirated, and cells in each well washed twice with sterile PBS. The washed cells were fixed by washing with methanol, followed by addition of 50 % glycerol. The fixed

Journal of Integrated Science and Technology

J. Integr. Sci. Technol., 2016, 4(2), 46-50   47

cells were then analysed using a fluorescence microscope (ZEISS Axiovert 40 CFL).

The quantitative estimation of uptake of nanophosphors (CP-EU, CP-EU-PA) in cells via fluorescence analysis of cell lysates was carried out by a similar procedure as above. Here, after nanoparticle treatment and subsequent washing of cells with PBS, as described above, the cells were lysed by adding 200 µl of cell lysis reagent (1 % Triton X- 100 in water) to each well of the 6-well plate, followed by incubation for 30 min with gentle shaking. After this, the cells in the lysis solution were scraped with a sterile scraper, and mixed with an additional 1 ml of PBS added to each well. Then, the mixture was transferred to microcentrifuge tubes (maximum capacity 1.5 ml). The cell debris was separated from the lysate by centrifugation (3,000 rpm, 5 min). The supernatant (centrifugate) was collected for analysis of nanophosphors fluorescence in the spectrofluorimeter.

RESULTS AND DISCUSSION

The TEM image of the synthesized doped calcium phosphate nanophosphors is shown in Figure 1 (A). The diameter of irregular 'grain like' shaped varied in the range of 30 to 50 nm.

The elemental composition of these nanophosphors, containing carbon, nitrogen, oxygen, silica, phosphorous, calcium and europium, confirms from the EDX analysis of the nanophosphors{as shown in Figure 1(B)}.
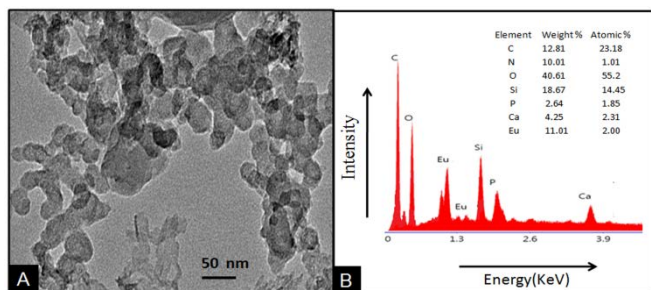

Figure 1. (A) TEM image of doped calcium phosphate nanophosphors (CP-EU), and (B) EDX data of doped phosphate nanophosphors (CP-EU).

The SAED diffraction pattern of the nanophosphors, presented in Figure 2(A), shows the sharp 002 diffraction peak reflecting the elongated nature of the crystals and the broad diffraction band containing the 211 and 300 diffraction peaks, along with some other small diffraction bands. These bands are characteristic of calcium phosphate nanoparticles[17]. These diffraction bands show that particles are crystalline in nature. Powder XRD patterns of the doped calcium phosphate nanophosphors are presented in Figure 2(B).

The data shows similar result, with the main peaks corresponding to $2\theta \approx 26^{o}$ (being 002 diffraction, d=3.427) and at $2\theta \approx 32^{o}$ (overlapping diffraction of 211, d211=2.805). FTIR This XRD pattern largely corresponds to that of hydroxyapatite (HA), which is the most common
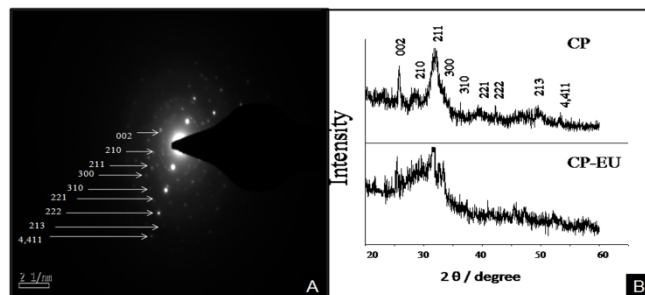

Figure 2. (A) Diffraction pattern of doped calcium phosphate nanophosphors (CP-EU), and (B) XRD spectra of CP (calcium phosphate nanoparticles) and CP-EU (doped calcium phosphate nanophosphors).

crystalline phase of calcium phosphate (standard JCPDS, #09-0432). It can be found that the relative intensities of the diffraction decrease in case of doped calcium phosphate nanophosphors. This is because doping inhibits the HA crystal growth. Overall, the poor crystalline nature of the doped calcium phosphate nanophosphors can be ascribed due to low temperature synthetic procedure[18]. The FTIR spectra of calcium phosphate (CP) and doped calcium phosphate nanophosphors (CP-EU) are presented in Figures 3. The characteristic FTIR absorption peaks of CP nanoparticles (in the hydroxyapatite form) are evident. The sharp peak around 3400 cm^{-1} was attributed due to the stretching vibration of the lattice OH- ions.[19-21]

The presence of PO_4^{3-} ions is indicated by characteristic bands appearing at 878 and 1095 cm^{-1}. The observation of the asymmetric P-O stretching vibration of the PO_4^{3-} band at 878 cm^{-1} as a distinguishable peak, together with sharp peaks around 594 and 698 cm^{-1}, corresponds to the O-P-O bending vibration of PO_4^{3-} in hydroxyapatite. Doublet in the range 1000-1100 cm^{-1} was assigned to P-O antisymmetric stretching mode.[22] These bands indicate the characteristic molecular structures of the polyhedrons of PO_4^{3-} in the hydroxyapatite lattice. An additional hump around 1400-1500 cm^{-1} corresponds to the mixing of the trisilanol moiety with the PO_4^{3-} formed during the CP nanoparticle formation. We observed that the contribution of the area that corresponds to the phosphate bands at 594 and 878 cm^{-1} progressively decreases in the presence of europium in case of nanophosphors. We can also observe in the Eu: Calcium phosphate spectra a broadening of peak vibration in the presence of the europium. This behavior was observed by Owada et al.[23] in sintered Y-doped hydroxyapatite.

The optical properties of aqueous solutions of doped calcium phosphate nanophosphors (CP-EU), and doped calcium phosphate nanophosphors co-doped with 1,10-Phenanthroline (CP-EU-PA), have been studied by excitation and fluorescence (photoluminescence) spectroscopies. The excitation spectrum was obtained by recording the $^{5}D_0 \rightarrow {}^{7}F_2$ emission of Eu^{3+} at 614 nm, as shown in Figure 4. The highest excitation peaks are observed at 250 nm and 394 nm, in the UV region. Besides, excitation in the visible region is possible at 484 nm. The broad peak at 250 nm was attributed to a charge transfer transition between Eu^{3+} and O^{2-}.[24-25]
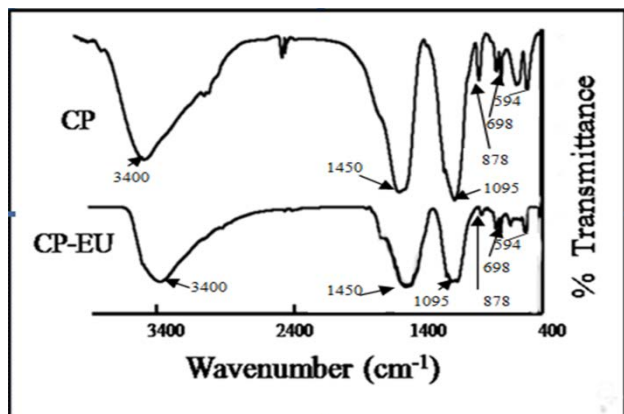
Journal of Integrated Science and Technology

J. Integr. Sci. Technol., 2016, 4(2), 46-50   48

Figure 3. FTIR spectra of CP (calcium phosphate nanoparticles) and CP-EU (doped calcium phosphate nanophosphors) only.
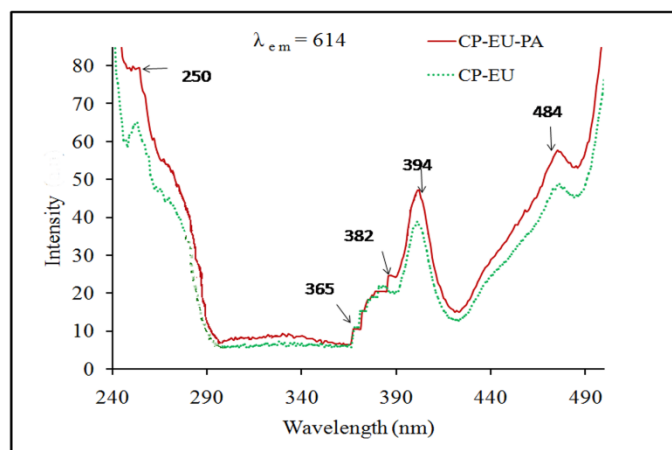

Figure 4. Excitation spectra of CP-EU, CP-EU-PA nanophosphors.

In the longer wavelength region, the weak peaks may arise from the direct excitation of the Eu^{3+} ground state into higher levels in the 4f6 configuration, which can be assigned to $^7F_0 \rightarrow {}^5H_6$ (320 nm), $^7F_0 \rightarrow {}^5D_4$ (365 nm), $^7F_0 \rightarrow {}^5G_2$ (382 nm), $^7F_0 \rightarrow {}^5L_6$ (398 nm), $^7F_0 \rightarrow {}^5D_2$ (484 nm), respectively.

Upon excitation at 394 nm, the characteristic transition lines from the excited $^5D_0$ level of Eu^{3+} ions can be detected in the emission spectra [26], as shown in Figure 5. The locations of the emission lines with their spectral assignments are labelled as well. Spectral features are observed in three different ranges: 570–582, 582–603, and 603–640 nm. They were ascribed to the $^5D_0 \rightarrow {}^7F_0$, $^5D_0 \rightarrow {}^7F_1$, and $^5D_0 \rightarrow {}^7F_2$ transitions, respectively. The $^5D_0 \rightarrow {}^7F0$ transition observed at 578nm is related to Eu^{3+} ions distributed on Ca^{2+} sites of the apatitic structure [27].

The two main characteristic peaks from $^5D_0 \rightarrow {}^7F_1$ (591 nm) and $^5D_0 \rightarrow {}^7F_2$ (614 nm) are dominant. The more efficient emission was observed for the hypersensitive $^5D_0$–$^7F_2$ transitions whose maximum intensity was obtained at 614 nm. An enhancement in the intensity of the peak after using 1, 10 phenanthroline as a co-dopant is due to the ligand-to-metal energy transfer.

Characteristic red luminescence of the Eu^{3+} ion can be observed at 614nm ($^5D_0 \rightarrow {}^7F_2$) in the emission spectra.
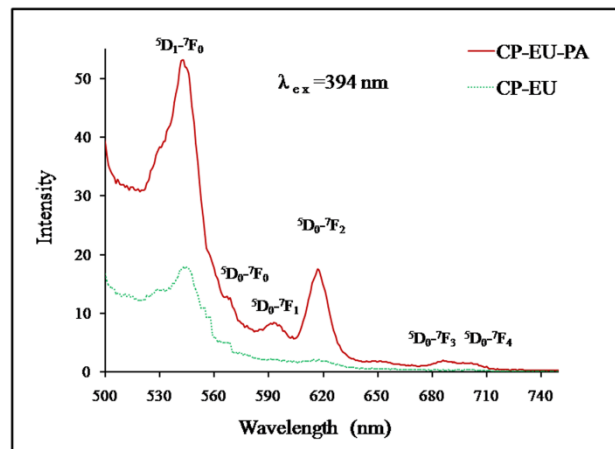

Figure 5. Luminescence spectra of CP-EU, and CP-EU-PA.

Therefore, the Eu^{3+} ion is excited via energy transfer from the initially excited organic ligand. The excitation energy is transferred from the triplet state of the ligand to the nearest lower resonance level of the Eu^{3+} ion.[28,29]

Following these characterization studies, we probed the interaction of these nanophosphors with cells in vitro, using A-549 cells. First, fluoresecence microscopy results qualitatively demonstrated the uptake of nanophosphors (CP-EU-PA), After that, we used spectrofluorimetric analysis of lysates of nanophosphors treated cells to quantitatively probe the cellular uptake of the nanoparticles. Here, cells were treated with CP-EU and CP-EU-PA. Figure 6 (A) shows higher fluorescence intensity from cells treated with CP-EU-PA, when compared to that of cells treated with CP-EU. Overall, the above experiment concluded that these nanophosphors are well uptaken by cells in vitro.

Next, in order to study the biocompatibility and non-cytotoxicity of the nanoparticles, we have treated A-549 cells with these nanoparticles (at three different dosages: high, medium and low) for two days, and analyzed the cell viability.

It can be seen from Figure 6 (B) that after 48 hours of nanophosphor treatment, the cells remained about 80-90 % viable in all the dosages tested, with relatively higher viability for the lower dosages. This data demonstrates that the nanophosphors exert negligible toxic effect on the cells, and have the potential to be used in biological applications.[30]
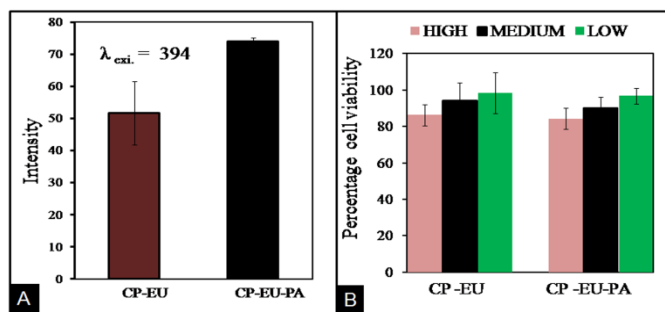

Figure 6. (A) Quantitative estimation of fluorescence recovered from lysates of cells treated with CP-EU and CP-EU-PA. (B) Cell viability (MTT) assay of CP-EU and CP-EU-PA (High: 100 µg/ml, Medium: 50 µg/ml, Low: 25µg/ml).

Journal of Integrated Science and Technology

J. Integr. Sci. Technol., 2016, 4(2), 46-50 49

CONCLUSIONS

In the present article we have explained the successful synthesis, satisfactory cell viability and cell uptake of doped calcium phosphate nanophosphors. Luminescence intensity of doped calcium phosphate nanophosphors is enhanced with the use of 1, 10- phenanthroline as a co-dopant. The synthesis was confirmed by several characterization methods, such as elemental analysis, FTIR, XRD, Fluorescence, etc. There was improvement in the luminescence intensity of the nanophosphors when 1, 10-phenanthroline was used as a co-dopant. Luminescence property of nanophosphors makes them viable optical trackers in the biological system.

REFERENCES

1 K.Y. Jung, H.W. Lee. Enhanced luminescent properties of $Y_3Al_5O_{12}$:Tb^{3+}, Ce^{3+} phosphor prepared by spray pyrolysis. *J. Lumin.,* **2007** , 126, 469-474.

2. A. M. Pires, O.A. Serra, M.R. Davolos. Morphological and luminescent studies on nanosized Er, Yb–Yttrium oxide up-converter prepared from different precursors. *J. Lumin.,* **2005**, 113, 174-182.

3. X. Y. Chen, H.Z. Zhuang, G.K. Liu, S. Li, R.S. Niedbala. Confinement on energy transfer between luminescent centers in nanocrystals. *J. Appl. Phys.*, **2003**, 94, 5559-5565.

4. Y. C. Kang, I. W. Lenngoro, S. B. Park, K. Okuyama. YAG: Ce phosphor particles prepared by ultrasonic spray pyrolysis. *Mat. Res. Bul*., **2000**, 35, 789-798.

5. H. Chang, I. W. Lenggoro, K. Okuyama, T. O. Kim. Nanoparticles of a doped oxide phosphor prepared by direct-spray pyrolysis. *Jpn. J. Appl. Phys.,* **2004**,43, 3535-3539 .

6. L. G. Jacobsohn, B.L. Bennett, R.E. Muenchausen, J.F. Smith, D. W. Cooke. Luminicent properties of nanophosphors. *Radi. Measur.,* **2007,** 42, 675-678.

7. S.K. Lee, H.H. Yoon, S.J. Park, K.H. Kim, H.W. Choi. Photoluminescence Characteristics of $Y_3Al_5O_{12}$:Ce^{3+} Phosphors Synthesized Using the Combustion Method with Various Reagents. *J. Appl. Phys.,* **2007**,46 , 7983-7986.

8. B.S. Chhikara, S. Kumar, N. Jain, A. Kumar, R. Kumar. Perspectivity of bifunctional chelating agents in chemical, biological and biomedical applications. *Chem. Biol. Lett.,* **2014**, 1(2), 77-103.

9. Y. Wan, L. Zhang, L. Lin, S. Gao, S. Lu. High-dimensional architectures from the self-assembly of lanthanide ions with benzenedicarboxylates and 1,10-phenanthroline. *Inorg. Chem.,* **2003**, 42, 4985-4994.

10. P. Lenaerts, C. Görller-Walrand, K. Binnemans. Luminescent europium(III) and terbium(III) nicotinate complexes covalently linked to a 1,10-phenanthroline functionalised sol–gel glass. *J. Lumin.,* **2006**, 117, 163-169.

11. M. Flores, U. Caldino, R. Arroyo. Luminescence properties of terbium doped poly(acrylic acid) containing 1,10-phenanthroline and 2,2^'-bipyridine . *Opt. Mater.,* **2006**, 28, 514-518.

12. L. Armelao, S. Quici, F. Barigelletti, G. Accorsi, G. Bottaro, M. Cavazzini, E. Tondello. Design of luminescent lanthanide complexes from molecule to highly efficient photo emitting materials. *Coord. Chem. Rev*., **2010**, 254, 487-505.

13. J. Ritchie, A. Ruseckas, P. André, C. Münther, M. Van Ryssen, D. E. Vize, J. A. Crayston, I. D. W. Samuel. Synthesis and lanthanide-sensing behaviour of polyfluorene/1,10-phenanthroline copolymers. *Synth. Met*., **2009**, 159, 583-588.

14. M. Fernandes, V. de Zea Bermudez, R. A. Sá Ferreira, L. D. Carlos, A. Charas, J. Morgado, M. M. Silva, M. J. Smith. Highly Photostable Luminescent Poly(ε-caprolactone)siloxane Biohybrids Doped with Europium Complexes. *Chem. Mater.,* **2007**, 19, 3892-3901.

15. F. J. Feher, T. A. Budzichowski, R. L. Blanski, K. J. Weller, and J. W. Ziller. Facile Syntheses of New Incompletely Condensed Polyhedral Oligosilsesquioxanes: $[(c-(C_5H_9)_7Si_7O_9(OH)_3]$, $[(c-(C_7H_{13})_7Si_7O_9(OH)_3]$, and $[(c-(C_7H_{13})_7Si_6O_7(OH)_4]$*Organometallics*, **1991**, 10, 2526-2528.

16. I. Roy, T. Y. Ohulchanskyy, H. E. Pudavar, E. J. Bergey, A. R. Oseroff, J. Morgan, T. J. Dougherty, and P. N. Prasad. Ceramic-based nanoparticles entrapping water-insoluble photosensitizing anticancer drugs: a novel drug-carrier system for photodynamic therapy. *J. Am. Chem. Soc.,* **2003**, 125, 7860-7865.

17. A. P. Evan, J.E. Lingeman, F. L. Coe, Y. Shao, J. H. Parks, S. B. Bledsoe, C. L. Phillips, S. Bonsib, E. M. Worcester, A. J. Sommer, S. C. Kim, W. W. Tinmouth , M, Grynpas. Crystal-associated nephropathy in patients with brushite nephrolithiasis. *Kidney International* ,**2005**, 67, 576-591.

18. J. Panyam and V. Labhasetwar. Biodegradable nanoparticles for drug and gene delivery to cells and tissue. *Adv. Drug Deliv. Rev.,* **2003**, 55, 329-347.

19. P. Zimmer and J. Kreuter. Microspheres and nanoparticles used in ocular delivery systems. *Adv. Drug Deliv. Rev.,* **1995**, 6, 61-73.

20. D. H. W. Hubert, M. Jung, P. M. Frederik, P. H. H. Bomans, J. Meuldijk, and A. L. German. Vesicle-Directed Growth of Silica. *Adv. Mater.,* **2000**, 12, 1286-1290.

21. H. P. Hentze, S. R. Raghavan, C. A. McKelvey, and E. W. Kaler. Silica hollow spheres by templating of catanionic vesicles. *Langmuir*, **2003**, 19, 1069-1074.

22. Z. Gen-Tao, Y. Qi-Zhi, N.Y. Jie. Impliction or bio mineralization *J. Gu, Am. Mineral.,* **2009**, 94, 293-302.

23. H. Owada, K. Yamashita, T. Umegaki, T. Kanazawa, and M. Nagai. Humidity-sensitivity of yttrium substituted apatite ceramics. *Solid State Ionics,* **1989**, 35, 401-404.

24. Y. Wang, X. Guo, T. Endo, Y. Murakami, and M. Ushirozawa. Identification of charge transfer (CT) transition in (Gd,Y)BO 3:Eu phosphor under 100-300 nm. *Journal of Solid State Chemistry,* **2004**, 177, 2242-22448.

25. C. X. Li, Z. W. Quan, J. Yang, P. Yang, and J. Lin. Highly uniform and monodisperse beta-NaYF(4):Ln(3^+) (Ln = Eu, Tb, Yb/Er, and Yb/Tm) hexagonal microprism crystals: hydrothermal synthesis and luminescent properties. *Inorganic Chemistry*, **2007**, 46, 6329-6337.

26. D. Shi, J. Lian , W. Wang et al., Luminescent carbon nanotubes by surface functionalization, *Advanced Materials,* **2006**, 18,189-193.

27. M. E. Fleet and Y. Pan. Site preference of Nd in fluorapatite $[Ca_{10}(PO_4)_6F_2]$, *Journal of Solid State Chemistry*, **1994**, 112, 78-81.

28. A. Sharma, D. Singh, I. Singh. Performance analysis of energy-efficient Emitting Diodes (WPLEDs) Proc. of ASID '2006,46-49.

29. S. Sardar, P. Kar, S.K. Pal. The Impact of Central Metal Ions in Porphyrin Functionalized ZnO/TiO2 for Enhanced Solar Energy Conversion. *J. Mat. NanoSci.*, **2014**, 1(1), 12-30.

30. I. Roy, Anuradha. Synthesis and characterization of iron phosphate NPs and applications in magnetically guided drug delivery. *J. Mat. NanoSci.*, **2016**, 3(1), 1-7.

Journal of Integrated Science and Technology

J. Integr. Sci. Technol., 2016, 4(2), 46-50   50